

Fig. 2 Flutter dynamic pressure vs chordwise natural frequency of a rectangular wing.

homogeneous. The measured value of the frequencies of Ref. 7 reveals that the plate was not homogeneous, its chordwise frequency being much less than that theoretically predicted for a square plate, i.e., it approaches the value for a plate with an aspect ratio 1:2.

In order to examine the tendency of this mode to flutter when coupling with the torsion mode, a small disturbance in the aerodynamic stiffness matrix is included. This disturbance is accomplished by introducing in the aerodynamic stiffness matrix a value for the element (3,2) which is equal to a negative percentage of the element (2,3). The result of the analysis is shown in Fig. 2 for various percentages. Notice that a 10% disturbance is equivalent to moving the nodal lines only 1% chordwise forward and an asymmetry of 5% in the deflection of the trailing edge in relation to the leading edge. Observe that only 1% disturbance without the aerodynamic damping shows evidence of this type of violent flutter. Figure 2 also shows the flutter parameters given in Ref. 1 for an analysis when only modes 2 and 3 are considered. Finally, it must be observed that values of $\Lambda_3 \leq 1$ are physically impossible, since the chordwise mode cannot be a graver mode than the torsion mode. This classical example has been analyzed in detail in order to show the importance of the accuracy in the mode shapes when used in flutter analysis and the adequacy of the mode coalescence theory to predict violent types of flutter.

Conclusions

A method has been presented for the solution of the flutter problem within the theory of mode coalescence. It has been shown that the solution of the complex eigenvalue problem can be avoided and the problem can be reduced to that of the solution of two simultaneous algebraic equations with the critical flutter parameters as unknowns. Numerical applications have been presented and the adequacy of the use of the mode coalescence theory has been discussed.

References

- ¹Bisplinghoff, R. L., and Ashley, H., *Principles of Aeroelasticity*, John Wiley, New York, 1962.
- ²Dowell, E. H., *Aeroelasticity of Plates and Shells*, Noordhoff International, Leyden, The Netherlands, 1974.
- ³Dowell, E. H., Curtiss, H. C. Jr., Scanlan, R. H., and Sisto, F., *A Modern Course in Aeroelasticity*, Sijhoff & Noordhoff, Alphen aan den Rijn, The Netherlands, 1978.
- ⁴Niblett, L. T., "A Guide to Classical Flutter," *Aeronautical Journal*, Nov. 1988, pp. 339-354.
- ⁵Collar, A. R., "The Expanding Domain of Aeroelasticity," *Journal of the Royal Aeronautical Society*, Vol. 50, Aug. 1946, pp. 613-636.
- ⁶Pipes, L. A., *Applied Mathematics for Engineers and Physicists*, McGraw-Hill, New York, 1958.
- ⁷Dugundji, J., and Crisp, J. D. C., "On the Aeroelastic Characteristics of Low Aspect Ratio Wings with Chordwise Deformation," OSR TN 59-787, July 1959.

Structural and Aerodynamic Data Transformation Using Inverse Isoparametric Mapping

R. M. V. Pidaparti*

Purdue University, Indianapolis, Indiana 46202

I. Introduction

FINITE element methods are being used in aeroelastic analysis to predict flutter boundaries, response, etc. In aeroelastic analysis, different discretization procedures are used for structural and aerodynamic parameters. For example, in MSC/NASTRAN, one set of discretization is based on aerodynamic theory and the other set of discretization is based on structural considerations. It is necessary to find the aerodynamic parameters at the structural grid and vice versa for aeroelastic analysis. For example, the structural deformations are required at the aerodynamic grid points and the aerodynamic loads are required at the structural grid points.

Several numerical procedures were developed to get the necessary information between the aerodynamic and the structural grids. These procedures employ a least squares technique for interpolation,¹ polynomial fit,² and spline functions based on simple beam and infinite plate equations.^{3,4} In Ref. 5, a piecewise cubic monotone interpolation scheme was used to determine the displacements and the slopes at the aerodynamic grid points by deriving a transformation matrix. However, in all of these procedures, a system of equations has to be solved to get the required information between the aerodynamic and structural grid points. For irregularly shaped structural or aerodynamic grids, the system of equations becomes ill conditioned and the results will be inaccurate.

The present approach is to use the inverse isoparametric mapping to transform the state variables such as displacement, load, stress, pressure, temperature, etc., from the structural grid points to aerodynamic grid points. The plane form of the wing can be represented by either four-node or eight-node isoparametric finite elements. Although the present approach is intended for interpolation between the two sets of grids, extrapolation to control surfaces, such as flaps, is possible by combining the well-known extrapolation techniques and inverse mapping procedure. The present approach is demon-

Received Jan. 27, 1990; revision received Oct. 15, 1990; accepted for publication Dec. 31, 1990. Copyright © 1991 by the American Institute of Aeronautics and Astronautics, Inc. All rights reserved.

*Assistant Professor, Department of Mechanical Engineering, School of Engineering and Technology, 723 W. Michigan Street.

strated for both interpolation and extrapolation between the structural and aerodynamic grids. The inverse mapping procedure is valuable and efficient in the aeroelastic data transformation because each state variable (displacement or slope) is interpolated using the same shape functions in the sense of isoparametric mapping.

II. Inverse Isoparametric Mapping

In isoparametric mapping, the same shape functions N are used to interpolate the geometry and the state variables. The isoparametric mapping is from a local coordinate (ξ, η) to a global coordinate (x, y) . The mapping is defined by the shape functions for an element:

$$x = \sum_{i=1}^n N_i(\xi, \eta) x_i \quad (1a)$$

$$y = \sum_{i=1}^n N_i(\xi, \eta) y_i \quad (1b)$$

where n is the number of nodes for the element.

The idea of inverse isoparametric mapping is to find a local coordinate (ξ_m, η_m) from the information given (x_m, y_m) in the global coordinates. The inverse mapping involves solving a system of nonlinear equations numerically using an iterative approach. In the present study, the approach of Ref. 6 is used to solve for the local coordinates (ξ_m, η_m) for the four-node and eight-node isoparametric finite elements. The inverse procedure is reviewed briefly in the following.

Consider an interior point $M(x_m, y_m)$ for which its local coordinates (ξ_m, η_m) are required. Define an arbitrary line PQ passing through the point M and any corner node P (see Fig. 1) whose coordinates are known. The line PQ transforms to $P'Q'$ through the inverse mapping. The local coordinates of M can be found using the shape functions and coordinates of the element containing the point M . The equation for the line $P'Q'$ can be written as

$$A\xi^2 + B\xi + C = 0 \quad (2)$$

where the constants A , B , and C are functions of the coordinates and shape functions of the finite element enclosing the point M . The explicit expressions for the coefficients A , B , and C can be found.⁶ The quadratic equation (2) is solved iteratively for the correct root such that the value of ξ is in the range $[-1, +1]$. It should be noted that $P'Q'$ should be defined for the whole range of the η axis $[-1, +1]$ before a bisection on $P'Q'$ is possible. Sometimes it is necessary to choose another corner node P or use a simple transformation to interchange the ξ and η axes so that the required values of η ($-1 \leq \eta \leq 1$) can be found.

After finding the local coordinates ξ_m and η_m , the state variable at the point M can be obtained using the isopara-

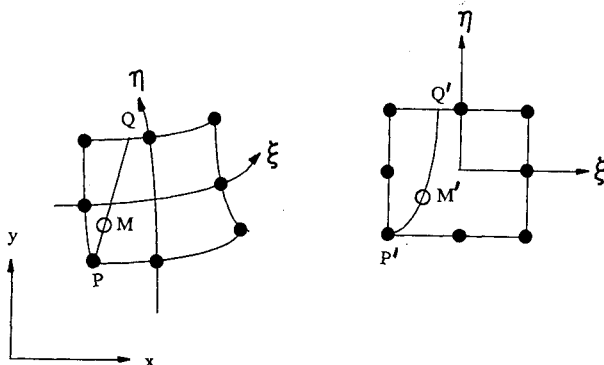


Fig. 1 Transformation of line PQ by inverse mapping.

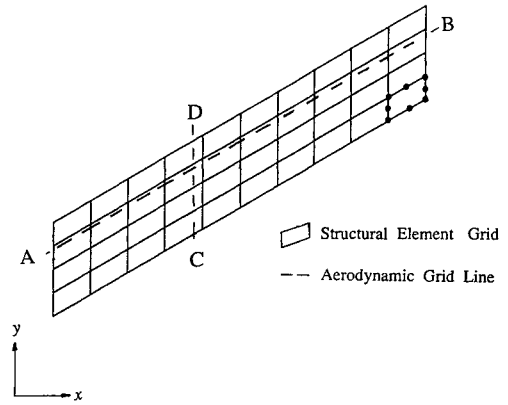


Fig. 2 Typical oblique wing with structural grid and aerodynamic grid line.

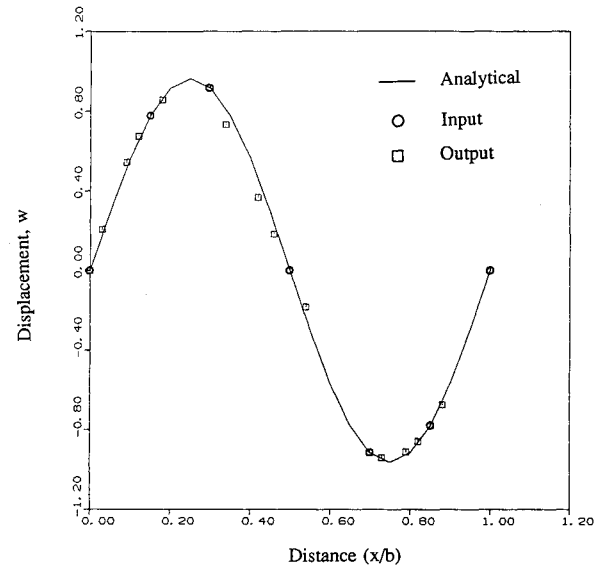


Fig. 3 Comparison of deformation along the aerodynamic grid line AB .

metric mapping as

$$\phi = \sum_{i=1}^n N_i(\xi, \eta) \phi_i \quad (3)$$

where ϕ is the state variable at any point in the element. This procedure has to be carried out by choosing the appropriate structural element containing the aerodynamic grid point in the mesh.

Although the present approach is intended for interpolation, extrapolation to the control surfaces is possible by considering an extrapolated grid enclosing the control surfaces. The grid over the control surfaces can be extrapolated using the well-known linear or quadratic or cubic spline techniques. Then using this extrapolated grid, the required information at the control surface points can be found using the inverse mapping procedure. However, the extrapolation is not as accurate as the interpolation.

III. Results and Conclusions

Consider a typical oblique wing, as shown in Fig. 2. Eight-node isoparametric finite elements were used to discretize the wing. Let the deformed shape of the wing be represented as

$$w = \cos(cy) \sin(bx) \quad (4)$$

where the constants b and c are chosen to give one full wave in the x and y directions, respectively. The displacements can be calculated at any point on the wing by using Eq. (4).

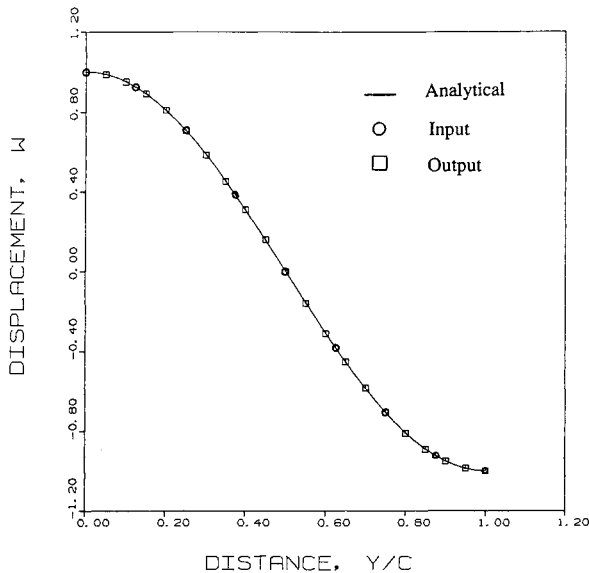


Fig. 4 Comparison of deformation along the aerodynamic grid line CD.

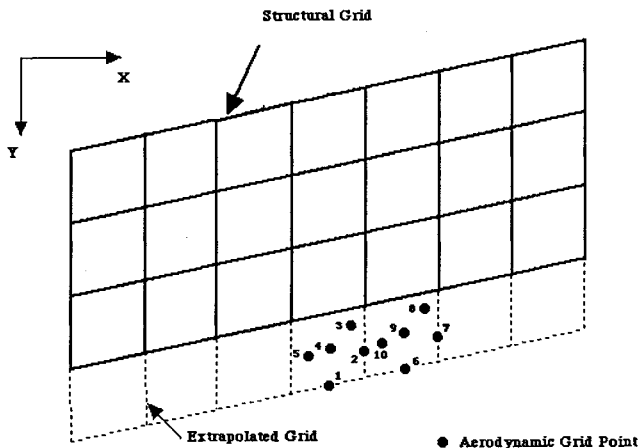


Fig. 5 Structural grid extrapolated to the control surfaces.

The displacements are calculated at the aerodynamic grid line AB by using three eight-node finite elements and the inverse mapping procedure. The displacements along the aerodynamic grid line AB are shown in Fig. 3 along with those calculated from Eq. (4). The solid line represents the displacements calculated using Eq. (4), and the circles represent the displacements used as inputs to the inverse mapping program. The square symbols denote the calculated displacement (output) from the inverse mapping procedure. It can be seen from Fig. 3 that the present results are in excellent agreement with the analytical solution. Similarly, the displacements calculated along the aerodynamic grid line CD using four eight-node finite elements for a constant value of x are shown in Fig. 4. Once again, a good agreement is found between the results obtained from the inverse mapping procedure and the analytical solution. Depending on the accuracy required, a larger number of elements are to be used for inverse mapping calculation along a particular aerodynamic grid point/line.

To show how the inverse mapping procedure can be used for obtaining the required data at the control surfaces/grid points, the problem shown in Fig. 5 was considered. The displacement for the problem shown in Fig. 5 is assumed as given by Eq. (4). The structural grid is extrapolated to the control surfaces using linear, quadratic, and cubic spline techniques. Using this extrapolated grid of two eight-node finite elements, the displacement is obtained at 10 different points over the control surface using the inverse mapping procedure. The percent error between the results from the inverse map-

Table 1 Percent error between the analytical solution and the inverse mapping procedure using different extrapolation schemes over the control surface grid points

Point Number	Linear	Quadratic	Cubic spline
1	1.53	0.00	0.00
2	1.07	0.16	0.00
3	0.81	0.15	0.07
4	0.97	0.13	0.01
5	0.92	0.08	0.06
6	1.53	0.30	0.00
7	1.08	0.16	0.00
8	1.09	0.43	0.35
9	0.97	0.13	0.01
10	0.76	0.08	0.22

ping and the analytical solution are summarized in Table 1 for different extrapolated schemes. It can be seen from Table 1 that the present approach gives the results with good accuracy.

Since isoparametric finite elements are used, any general wing configuration can be discretized. The inverse mapping procedure can be added to any of the existing finite element programs without any difficulty. The results presented indicate that the inverse mapping procedure is very accurate and efficient and, therefore, can be used for transforming any state variable (pressure, temperature, strain, etc.) between the aerodynamic and the structural grids.

References

- ¹Schmitt, A. F., "A Least Squares Matrix Interpolation of Flexibility Influence Coefficients," *Journal of the Aeronautical Sciences*, Vol. 23, Oct. 1956, pp. 980.
- ²Rodden, W. P., "Further Remarks on Matrix Interpolation of Flexibility Influence Coefficients," *Journal of the Aerospace Sciences*, Vol. 26, Nov. 1959, pp. 760-761.
- ³Done, G. T. S., "Interpolation of Mode Shapes: A Matrix Scheme Using Two-Way Spline Curves," *Aeronautical Quarterly*, Vol. XVI, Nov. 1965, pp. 333-349.
- ⁴Harder, R. L., and Desmarais, R. N., "Interpolation Using Surface Splines," *Journal of Aircraft*, Vol. 9, No. 2, 1972, pp. 189-191.
- ⁵Appa, K., Yankulich, M., and Cowan D. L., "The Determination of Load and Slope Transformation Matrices for Aeroelastic Analysis," *Journal of Aircraft*, Vol. 22, No. 8, 1985, pp. 734-736.
- ⁶Murti, V., and Vallippan, S., "Numerical Inverse Isoparametric Mapping in Remeshing and Nodal Quantity Contouring," *Computers and Structures*, Vol. 22, No. 6, 1986, pp. 1011-1021.

Effect of Thrust Vectoring on Level-Turn Performance

Pai-Hung Lee*

Aeronautical Research Laboratory,
Taichung, Taiwan 40722, Republic of China
and

C. Edward Lan†

University of Kansas, Lawrence, Kansas 66045

Introduction

IN recent years, thrust vectoring has been actively considered as a means to improve a fighter's performance. Most

Received Nov. 8, 1990; revision received Jan. 4, 1991; accepted for publication March 8, 1991. Copyright © 1991 by the American Institute of Aeronautics and Astronautics, Inc. All rights reserved.

*Section Head.

†Professor, Aerospace Engineering. Associate Fellow AIAA.